

REPORT

ASTEROID BELT

Identification of a primordial asteroid family constrains the original planetesimal population

Marco Delbo^{1,*}, Kevin Walsh², Bryce Bolin¹, Chrysa Avdellidou³, Alessandro Morbidelli¹

A quarter of known asteroids is associated with more than 100 distinct asteroid families, meaning that these asteroids originate as impact fragments from the family parent bodies. The determination of which asteroids of the remaining population are members of undiscovered families, or accreted as planetesimals from the protoplanetary disk, would constrain a critical phase of planetary formation by unveiling the unknown planetesimal size distribution. We discovered a 4-billion-year-old asteroid family extending across the entire inner part of the main belt whose members include most of the dark asteroids previously unlinked to families. This allows us to identify some original planetesimals, which are all larger than 35 kilometers, supporting the view of asteroids being born big. Their number matches the known distinct meteorite parent bodies.

Understanding the formation of the planetesimals, the building blocks of planets, is a crucial problem in planetary science. Traditionally, a coagulation process is invoked, in which accreting collisions create bodies of all sizes up to several hundreds of kilometers (*1*). However, new models propose that planetesimals can form preferentially as 10^2 to 10^4 km in size directly from the clumping of dust particles in the protoplanetary disk, essentially skipping the formation of kilometer-sized and smaller bodies (*1–4*). However, the resulting planetesimal size distribution predicted by these new models depends on the resolution of the simulations and therefore is not yet known quantitatively (*1, 5, 6*).

An alternative approach is to observationally constrain the original size distribution of planetesimals left in the main asteroid belt. Unfortunately, 4.5 billion years of collisions have broken up several original asteroids (the planetesimals) and produced generations of younger asteroid fragments, so the original size distribution can no longer be distinguished from that produced by collisions (*7*). In principle, the fragments of asteroids should be identifiable as asteroid families: clumps in orbital space with a significantly higher density than that of the local background (*8, 9*). However, these families disperse with time; each fragment's orbital proper semimajor axis (*a*) drifts because of thermal radiation force by the Yarkovsky effect (*10*), whereas

the eccentricity (*e*) and inclination (*i*) are affected by orbital resonances with the planets, the locations of which are crossed by the asteroids as they drift through the belt. This makes families more difficult to identify as they age because their members spread in (*a, e, i*) space so that they become confused with the background (*11–13*). The scattering of family fragments is further complicated by the fact that at some point in the solar system history, the giant planets suffered an orbital instability (*14*). This shifted the positions of the resonances and resulted in the incoherent dispersion of *e* and *i* of any pre-existing primordial (*12*) asteroid family in the main belt (*15*). All these effects are such that families older than 2.0 billion to 2.5 billion years are rarely identified compared with younger ones, implying that the sample of known families is observationally incomplete (*12, 13, 16*).

We searched for old and dispersed asteroid families using a method (*17, 18*) that seeks to identify V-shaped groups of asteroids in (*a, 1/D*) space, where *D* is the asteroid diameter (Fig. 1). A V-shape feature is the expected signature of an asteroid family created by the fragmentation of a single parent body (*10*) followed by the subsequent drift of the fragments' *a*-value from the family center because of the nongravitational Yarkovsky force, which occurs at a rate da/dt (*t* is the time) proportional to the inverse diameter, $1/D$. We applied our V shape searching method to asteroids with low geometric visible albedo $p_V < 0.12$ (fig. S1 and data S1) located in the inner main belt: $2.1 < a < 2.5$ astronomical units (AU), and $\sin i \leq 0.3$. This albedo threshold

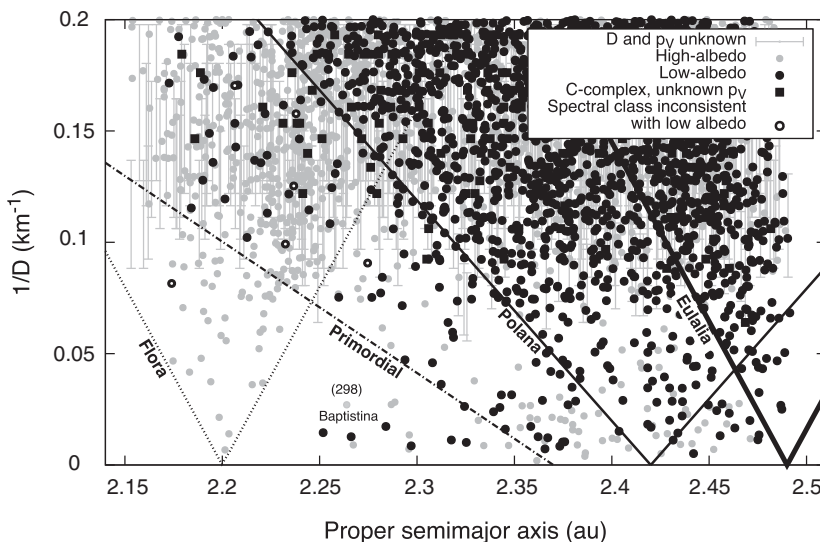


Fig. 1. Distribution of asteroids larger than 5 km in the inner main belt. The dotted lines, converging at 2.2 AU, delimit the high-albedo Flora family. Its V-shaped slope, $|K| = \sqrt{p_V}/1329/C = 1.6 \text{ km}^{-1} \text{ AU}^{-1}$, is derived from the *C* value of reference (*8*) with family's average geometric visible albedo $p_V = 0.28$ (*18*). Below the dashed-dotted line ($K = -0.59 \text{ km}^{-1} \text{ AU}^{-1}$), there is a void containing few low-albedo asteroids, with no dark bodies with $D < 50$ km, with the exception of the $D \sim 12$ km asteroid (1492) Opatz. This asteroid is classified in the S-complex (*19*) on the basis of its visible-light colors (*28*), and it belongs to the high-albedo Flora family, which are two indications that its $p_V = 0.09 \pm 0.03$ could be underestimated. The high-albedo asteroids inward of the primordial family border are either inside the V shape of the Flora family or have $D > 35$ km. The size of (298) Baptistina is conservatively corrected by adding the volume of its family members (*18*). For those asteroids with unknown *D*, we plot error bars whose limits are obtained by calculating their diameters from $D(\text{km}) = 1329/\sqrt{p_V} \times 10^{-H/5}$, where *H* is the absolute magnitude from (*29*). The upper and lower limit are given by assuming $p_V = 0.12$ and 0.05 , respectively. However, very few of these unknown-diameter objects could be located in the void.

preferentially selects asteroids with carbonaceous composition (18), classified in the spectroscopic C-complex (fig. S1) (19). We found a previously unidentified V shape (Fig. 2), whose inward side is visible in Fig. 1. The outward side is also located by our V shape searching method (18), but its detection is weak because it overlaps with the V shapes of other known families (fig. S2). The time at which the family formed is determined from the slope (12) of the inward side of its V shape to be $4.0^{+1.7}_{-1.1}$ billion years ago, making it older than most known families (Fig. 2 and fig. S3) (8, 12, 16, 18).

To check the reality of the newly identified primordial family, we first investigated the homogeneity of the physical properties of its members because the albedo and spectra are expected to be similar for asteroids that share an origin from a common parent body; this is often used to eliminate family interlopers (20). Next, we assessed the family's statistical significance (9). In the region of $(a, 1/D)$ space that is specific to the V shape detected here (the section of space between its inward border and that of the Polana family) (Fig. 1), the albedo distribution of the 125 dark asteroids matches that of the spectroscopic C-complex (fig. S4). Of the objects with known spectral classes, 17 out of 19 belong to the C-complex (table S1), and the variation in their visible wavelength spectra (fig. S5) is similar to that of other low-albedo families (20). The largest and lowest-numbered asteroid of this population is (51) Nemausa. In the region where members of the primordial family overlap those of other known families (18), in addition to the detection of the outward V-shape border (fig. S2), we also used a procedure (18) based on matching the size distribution, albedo, and spectra (Fig. 3 and figs. S4 and S5) to show that all 64 low-albedo asteroids with $D \geq 13$ km in the inner main belt and not associated to other families could also be members of the 4-billion-year-old family.

The V shape of the primordial family is not an over-density of asteroids above a diffuse background, which is typical for younger families (9). Instead, the inward edge of the V shape marks the border of a triangular void of dark asteroids, with $2.15 < a < 2.366$ AU and $0.02 < 1/D < 0.125$ km⁻¹ ($50 > D > 8$ km) (Fig. 1). There is only one asteroid—but likely misclassified as low-albedo, with $a = 2.174$ AU and $1/D = 0.081$ km⁻¹ (data S1)—in the void. Because of the absence of background, we needed to develop methods to assess statistical significance of the void and the V shape. First, we performed a series of tests (18) that show that the probability is smaller than 10^{-6} to produce from size-independent distributions of asteroid orbital semimajor axes a V shape and a void similar to those formed by low-albedo asteroids. Next, we tested whether the void of asteroids and the primordial V shape could be the results of 4 billion years of dynamical evolution of an initially random distribution of bodies. We did this by investigating whether the weak orbital resonances with the planets—that asteroids may cross as their semi-

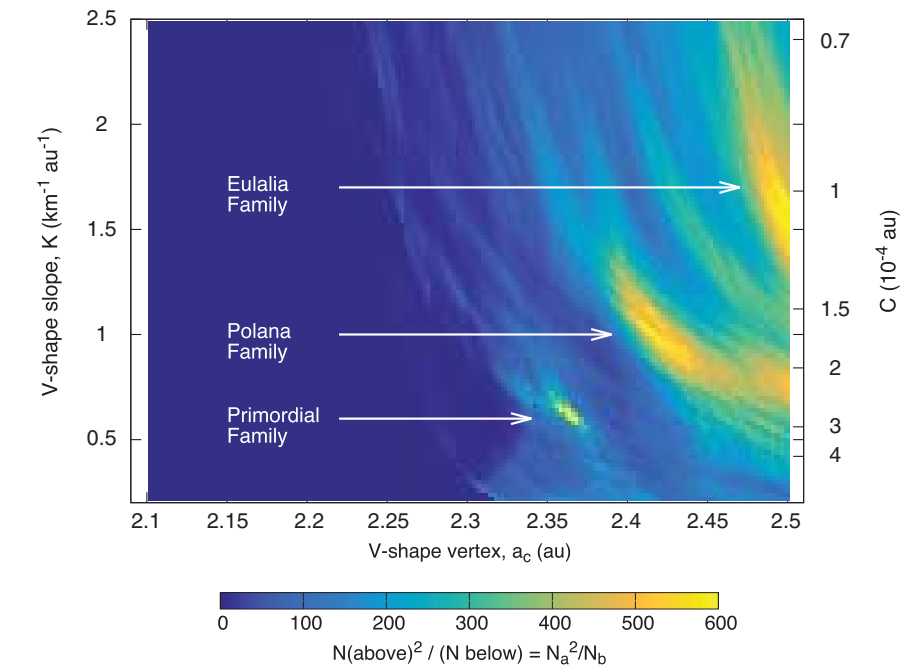


Fig. 2. Output of the V shape searching method. The value of N_a^2/N_b is shown in color as a function of the slope (K) and semimajor axis of the vertex of a V shape (a_c). Maxima in this quantity correspond to probable families because of an excess of the value of N_a^2/N_b above its local background (18). The high values of the output at $a_c = 2.49$ AU with $|K| \sim 1.7$ km⁻¹ AU⁻¹ and $a_c = 2.42$ AU with $|K| \sim 1.1$ km⁻¹ AU⁻¹ correspond to ages of ~ 1 billion years and ~ 1.9 billion years, respectively (18). These are the previously identified families of Eulalia and Polana (30) [the “New Polana” of (30) is called “Polana” in this work]. The V shape of the primordial family has $a_c = 2.366$ AU, with a slope of $|K| \sim 0.59$ km⁻¹ AU⁻¹ giving an age of ~ 4 billion years. The value of the parameter C (10) is calculated from $C = 1/K\sqrt{p_V}/1329$ by using a geometric visible albedo $p_V = 0.055$ (fig. S4).

major axis drifts because of the Yarkovsky effect—can increase orbital eccentricities to extreme values, removing enough asteroids (27) to create the void, whose width depends on the asteroid size. We carried out numerical integrations of orbital evolution of asteroids over 4 billion years, including the Yarkovsky effect, the planets, and the major asteroids on their current orbits (18). We found that only $\sim 50\%$ of the initial asteroids were removed, with no preference for removing asteroids from the location of the void. Therefore, this process is not able to reproduce the observations, implying that there is no dynamical reason for the presence of the void (fig. S6).

The few dark asteroids below the void (Fig. 1), inward and outside of the border of the primordial family, have $D > 50$ km. Similarly, the high-albedo objects in the same region of space that are not included in other family V shapes have $D > 35$ km. We conclude that the inner main belt contains asteroids of two different origins: (i) those that are collisional fragments of other asteroids and are inside V shapes and (ii) those that are outside V shapes, indicating that these original asteroids were not created as collisional fragments in the main belt and are, therefore, planetesimals accreted directly from the protoplanetary disk. This planetesimal population has only $D > 35$ km bodies and a

shallow size distribution (Fig. 4), implying that asteroids accreted big. This supports theoretical studies of the collisional evolution of the main belt (14), which indicated a preferred initial size of $D \sim 100$ km. To constrain the original population of planetesimals, the currently observed planetesimal population must be corrected for the size-dependent loss of bodies due to collisional and Yarkovsky-driven dynamical evolution. We computed an upper limit for the original size distribution of the planetesimals, taking into account asteroid loss as a stochastic process (18). The resulting original size distribution (Fig. 4) is still shallower than that predicted by some current accretion models (5, 22). The distribution could be even shallower if we consider a less effective collisional environment for the catastrophic destruction of asteroids (fig. S7).

We identified 17 primordial asteroids between 2.20 and 2.33 AU, totalling 170 when scaled to the entire range of the main belt (2.2 to 3.5 AU). This is very similar to the estimated number, 100 to 150, of the compositionally distinct parent bodies that are represented in the whole meteorite collection (23).

The origin of asteroids not associated with families, previously viewed as a background, has never been clearly identified (14). Our results show that the extent of the primordial family

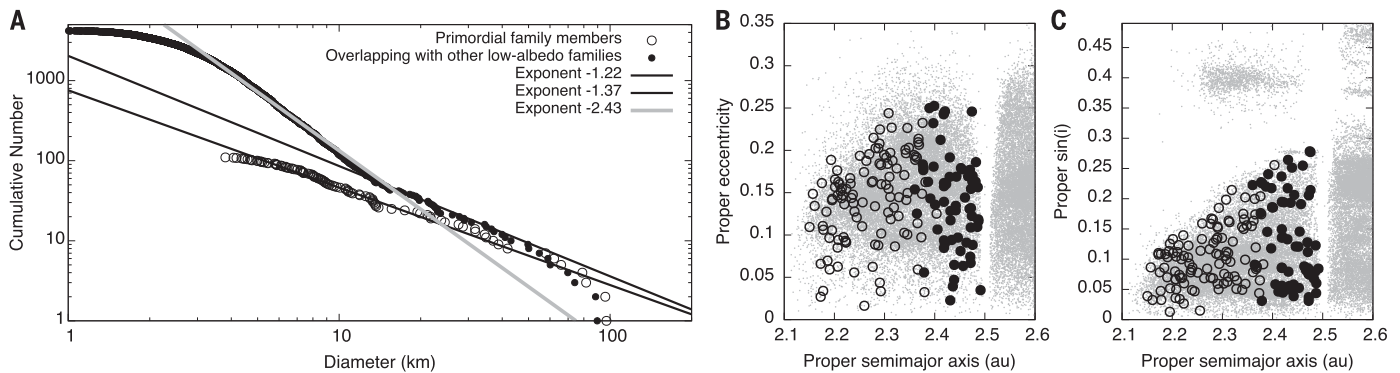


Fig. 3. Size distributions and spread in proper eccentricity and inclination of the primordial family members. (A) Cumulative size distributions of low-albedo asteroids located in the section between the inward borders of the primordial family V shape and the Polana family (open circles), and low-albedo asteroids that do not belong to other families in the region of $(a, 1/D)$ space above and beyond the inward border of the Polana family (solid circles). There are no known asteroids with $D < 3.82$ km in

the first population. The slope of the size distribution of the second population changes at $D \sim 13$ km. (B and C) Orbital distribution of primordial family members, which are spread over the entire inner main belt. For the first (open circle) population, only asteroids with $D < 50$ km are displayed in (B) and (C). For the second (solid circles) population, only objects with $13 < D < 50$ km are plotted. Gray dots represent all other known asteroids, regardless of their albedo values.

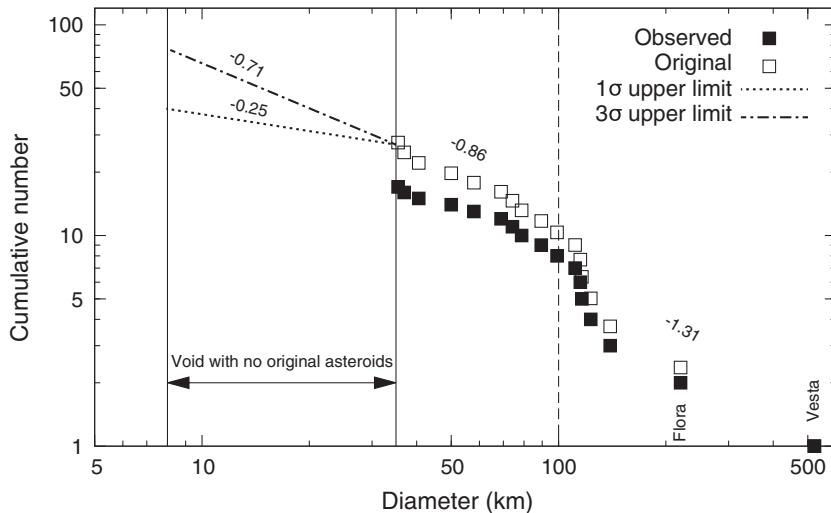


Fig. 4. Cumulative size distribution of planetesimals. The cumulative size distribution of those asteroids that are outside V shapes unless they are family parents, such as (8) Flora (solid squares), is corrected for the maximum number of objects that were lost because of the collisional and dynamical evolution, in order to obtain an upper limit for the distribution of the planetesimals (open squares). Functions of the form $N(> D) = N_0 D^\beta$, where N is the cumulative number of asteroids, are fitted piecewise in the size ranges $D > 100$ km, $35 < D < 100$ km, and $8 < D < 35$ km. For the original planetesimals size distribution, we obtain the values of β reported by the labels in the plot. In the range of sizes between 8 and 35 km, we give the 1σ and the 3σ upper limits on the planetesimals size distribution. The sizes of (8) Flora, (27) Euterpe, and (298) Baptistina are conservatively corrected by adding the volume of their respective family members (18).

and that of the other known low-albedo families covers the entirety of the inner main belt. This means that all dark asteroids with $D < 50$ km in that region are likely members of the primordial or other families. The implication is that the background of unaffiliated asteroids is represented only by the planetesimals, whereas the smaller low-albedo asteroids could be linked back to a handful of original inhabitants. We suspect that this could be a general feature of the main belt, which we have shown here only for $2.1 < a < 2.5$ AU.

Unlike other old families, the eccentricity and inclination of the primordial family members are not correlated, spanning the entire orbital element space of the inner main belt (Fig. 3, B and C). The e and i distributions of the members of the primordial family are similar to models of families that may have formed before the giant planet instability (15). The precise time of onset of the instability remains the object of discussion and ongoing research (24), but our results indicate that this family predates the instability regardless

of its date because the calculated Yarkovsky drift age allows the family to be as old as the solar system. Although there is evidence for this instability throughout the solar system (14), the primordial family represents a record of the collisional evolution of the main belt before this event. The existence of this family implies that the main belt before the planetary instability was sufficiently dynamically excited to produce at least one very large family-forming collision (25).

Some of the largest members of the other known low-albedo families are within the boundaries of the primordial family (fig. S2). Therefore, these other parents could have been family members of the primordial family themselves, before suffering their own subsequent family-forming collision. This includes families for which spectral surveys found similarities and homogeneities across their members in multiple wavelength regimes (20, 26, 27). If some of the other low-albedo families are related to the primordial family, then a large fraction of all low-albedo

asteroids in the inner main belt could share a common parent.

REFERENCES AND NOTES

1. A. Johansen, E. Jacquet, J. N. Cuzzi, A. Morbidelli, M. Gounelle, in *Asteroids IV*, P. Michel et al., Eds. (Univ. Arizona Press, 2015), pp. 471–492.
2. A. N. Youdin, J. Goodman, *Astrophys. J.* **620**, 459–469 (2005).
3. A. Johansen et al., *Nature* **448**, 1022–1025 (2007).
4. J. N. Cuzzi, R. C. Hogan, K. Shariff, *Astrophys. J.* **687**, 1432–1447 (2008).
5. J. B. Simon, P. J. Armitage, R. Li, A. N. Youdin, *Astrophys. J.* **822**, 55 (2016).
6. H. Klahr, A. Schreiber, *Proc. Int. Astron. Union* **318**, 1 (2016).
7. W. F. Bottke et al., in *Asteroids IV*, P. Michel et al., Eds. (Univ. Arizona Press, 2015), pp. 701–724.
8. D. Nesvorný, M. Brož, V. Carruba, in *Asteroids IV*, P. Michel et al., Eds. (Univ. Arizona Press, 2015), pp. 297–321.
9. A. Milani et al., *Icarus* **239**, 46–73 (2014).
10. D. Vokrouhlický, M. Brož, W. F. Bottke, D. Nesvorný, A. Morbidelli, *Icarus* **182**, 118–142 (2006).
11. A. Parker et al., *Icarus* **198**, 138–155 (2008).
12. F. Spoto, A. Milani, Z. Knežević, *Icarus* **257**, 275–289 (2015).
13. V. Carruba, D. Nesvorný, S. Aljbaae, R. C. Domingos, M. Huaman, *Mon. Not. R. Astron. Soc.* **458**, 3731–3738 (2016).
14. A. Morbidelli, K. J. Walsh, D. P. O'Brien, D. A. Minton, W. F. Bottke, in *Asteroids IV*, P. Michel et al., Eds. (Univ. Arizona Press, 2015), pp. 493–507.

15. P. I. O. Brasil *et al.*, *Icarus* **266**, 142–151 (2016).
16. M. Brož, D. Vokrouhlický, A. Morbidelli, D. Nesvorný, W. F. Bottke, *Mon. Not. R. Astron. Soc.* **414**, 2716–2727 (2011).
17. B. T. Bolin, M. Delbo, A. Morbidelli, K. J. Walsh, *Icarus* **282**, 290–312 (2017).
18. Materials and methods are available as supplementary materials.
19. The spectra of asteroids are divided into the C-, S-, and X-complexes. Each complex is separated into classes. The C-complex includes asteroids that display reflectance spectra with weak or no features and with flat or very moderate slopes. The C-complex asteroids are historically associated to carbonaceous chondrite meteorites. The S-complex includes asteroids with absorption bands typical of ordinary chondrites, with iron and silicate compositions. The X-complex is characterized by moderately sloped spectra with no or weak features. It is compositionally degenerate because it contains objects with high and low albedos. The low-albedo X-complex asteroids could be compositionally similar to those of the C-complex.
20. J. de León *et al.*, *Icarus* **266**, 57–75 (2016).
21. D. A. Minton, R. Malhotra, *Icarus* **207**, 744–757 (2010).
22. A. Johansen, M. M. Low, P. Lacerda, M. Bizzarro, *Sci. Adv.* **1**, e1500109 (2015).
23. T. H. Burbine, T. J. McCoy, A. Meibom, B. Gladman, K. Keil, in *Asteroids III*, W. F. Bottke Jr., A. Cellino, P. Paolicchi, R. P. Binzel, Eds. (Univ. Arizona Press, 2002), pp. 653–667.
24. W. F. Bottke *et al.*, *Nature* **485**, 78–81 (2012).
25. B. C. Johnson, K. J. Walsh, D. A. Minton, A. N. Krot, H. F. Levison, *Sci. Adv.* **2**, e1601658 (2016).
26. J. R. Masiero *et al.*, *Astrophys. J.* **770**, 7 (2013).
27. N. Pinilla-Alonso *et al.*, *Icarus* **274**, 231–248 (2016).
28. F. E. DeMeo, B. Carry, *Icarus* **226**, 723–741 (2013).
29. The Minor Planet Center of the International Astronomical Union; Asteroid identification and orbital elements are obtained from the MPCORB.DAT file at www.minorplanetcenter.net/iau/MPCORB.html; accessed August 2016.
30. K. J. Walsh, M. Delbo, W. F. Bottke, D. Vokrouhlický, D. S. Lauretta, *Icarus* **225**, 283–297 (2013).

ACKNOWLEDGMENTS

M.D. and B.B. acknowledge support from the French National Program of Planetology. M.D. carried out part of this work while visiting the European Space Agency/European Space Research and Technology Centre and the Leiden Observatory (Netherlands).

K.W. was supported by the National Science Foundation, grant 1518127, and by the Bonus Qualité Recherche of the Observatoire de la Côte d'Azur (OCA). A.M. acknowledges support from the French National Research Agency, grant ANR-13-BS06-0003. Our asteroid database, including family assignments, is released as supplementary data S1. The software used for this work, the relevant input files, and our modified version of SWIFT_RMVS3, used for the dynamical analysis, are available at <https://dataverse.harvard.edu/dataverse/PrimordialFamily> (doi: 10.7910/DVN/MNA7QG, Harvard Dataverse). Comments of anonymous reviewers substantially improved this work.

SUPPLEMENTARY MATERIALS

www.sciencemag.org/content/357/6355/1026/suppl/DC1
Materials and Methods
Figs. S1 to S7
Table S1
References (31–65)
Data S1

19 December 2016; accepted 13 July 2017
Published online 3 August 2017
10.1126/science.aam6036

Identification of a primordial asteroid family constrains the original planetesimal population

Marco Delbo', Kevin Walsh, Bryce Bolin, Chrysa Avdellidou and Alessandro Morbidelli

Science **357** (6355), 1026-1029.

DOI: 10.1126/science.aam6036originally published online August 3, 2017

Family ties reveal original planetesimals

The asteroid belt originated from leftover debris from the formation of our solar system, including objects that never grew big enough to become planets. Destructive collisions led to the present proliferation of asteroids; groups that were initially part of the same body have related orbits and are known as families. Delbo' *et al.* identified an ancient family mostly consisting of dark asteroids that previously had not been linked to families (see the Perspective by DeMeo). From this, they calculated the original population of the belt, showing that it contained several dozen midsized bodies known as planetesimals.

Science, this issue p. 1026; see also p. 972

ARTICLE TOOLS

<http://science.sciencemag.org/content/357/6355/1026>

SUPPLEMENTARY MATERIALS

<http://science.sciencemag.org/content/suppl/2017/08/02/science.aam6036.DC1>

RELATED CONTENT

<http://science.sciencemag.org/content/sci/357/6355/972.full>

REFERENCES

This article cites 50 articles, 3 of which you can access for free
<http://science.sciencemag.org/content/357/6355/1026#BIBL>

PERMISSIONS

<http://www.sciencemag.org/help/reprints-and-permissions>

Use of this article is subject to the [Terms of Service](#)